

# Dependence of Gas Phase Abundances in the ISM on Column Density

B.P. Wakker, J.S. Mathis  
Department of Astronomy, University of Wisconsin  
475 N Charter St, Madison, WI 53706, USA  
wakker@astro.wisc.edu, mathis@astro.wisc.edu

## ABSTRACT

Sightlines through high- and intermediate-velocity clouds allow measurements of ionic gas phase abundances,  $A$ , at very low values of H I column density,  $N(\text{H I})$ . Present observations cover over 4 orders of magnitude in  $N(\text{H I})$ . Remarkably, for several ions we find that the  $A$  vs  $N(\text{H I})$  relation is the same at high and low column density and that the abundances have a relatively low dispersion (factors of 2–3) at any particular  $N(\text{H I})$ . Halo gas tends to have slightly higher values of  $A$  than disk gas at the same  $N(\text{H I})$ , suggesting that part of the dispersion may be attributed to the environment. We note that the dispersion is largest for Na I; using Na I as a predictor of  $N(\text{H I})$  can lead to large errors.

Important implications of the low dispersions regarding the physical nature of the ISM are: (a) because of clumping, over sufficiently long pathlengths  $N(\text{H I})$  is a reasonable measure of the *local* density of *most* of the H atoms along the sight line; (b) the destruction of grains does not mainly take place in catastrophic events such as strong shocks, but is a continuous function of the mean density; (c) the cycling of the ions becoming attached to grains and being detached must be rapid, and the two rates must be roughly equal under a wide variety of conditions; (d) in gas that has a low average density the attachment should occur within denser concentrations.

*Subject headings:* ISM: clouds, ISM, Abundances Galaxy: halo, Galaxy: disk

## 1. Introduction

The study of elemental abundances in the interstellar medium has a long history, both in the optical and with space-based UV spectrographs, such as *Copernicus* and the Hubble Space Telescope (*HST*). These studies show that most elements have apparent abundances relative to hydrogen substantially below those in the Sun. This is interpreted as due to depletion of ions onto dust grains.

Savage & Sembach (1996a) summarized high-quality abundance studies based on *HST* data. They concluded that the depletion of an element depends on the nature of the interstellar medium along the sightline. In cold, dense disk gas, S has near-solar abundance, while Si, Mg, Mn, Cr, Fe and Ni are progressively more depleted. In warm-disk gas, the gas-phase abundances appear higher than in the cool gas, while in halo gas they are even larger.

Jenkins, Savage & Spitzer (1986) used *Copernicus* to measure accurate column densities for Mg II, P II, Cl I, Cl II, Mn II and Fe II, for stars with distances,  $d$ , between 0.1 and 2 kpc. They measured  $N(\text{H I})$  from the damping wings of  $\text{Ly}\alpha$  and found a relation between the ionic abundance relative to H I,  $A$ , and the average density,  $\langle n_{\text{H}} \rangle$  ( $\equiv N(\text{H I})/d$ ). An explanation was provided by Spitzer (1985), who suggested that the observed depletion in a line of sight depends on the fraction of warm and cold (dense) gas encountered, where each component has a specific gas phase abundance of each ion.

Crinklaw, Federman, & Joseph (1994) observed Ca II and Ti II toward 12 stars with distances between 150 and 650 pc. The slope of the relation between  $\log[\langle n_{\text{H}} \rangle]$  and  $\log[A(\text{ion})]$  is similar for Ca II and Ti II, but it differs from those for Fe II, Mn II, Mg II and P II. They proposed that Ca II and Ti II mostly occur in the warm intercloud medium, and that the apparent depletion is very sensitive to the inclusion of high-density regions (with high depletion) in the sightline.

These studies were limited to sightlines with  $N(\text{H I})$  in the range  $10^{20}$  to  $7 \times 10^{21} \text{ cm}^{-2}$ . To extend this range, we used the high- and intermediate-velocity gas (HVCs and IVCs, see Kuntz & Danly 1996, Wakker & van Woerden 1997, Wakker 2000). In 21-cm emission these stand out in velocity from gas in the Milky Way disk, so that weak components (down to  $10^{18} \text{ cm}^{-2}$ ) can be measured. At low velocities, parcels of gas with such low column densities can not be separated from other high column density concentrations in the line of sight.

Wakker (2000) analyzed all the published absorption-line data pertaining to the high- and intermediate-velocity gas. Improved H I column densities (and thus improved ion abundances) were determined for about 250 sightlines. Ca II was measured for 97 components, Ti II for 6, Fe II for 13, Mn II for 5, Mg II for 10, and Na I for 34 (low-velocity Na I was taken from Ferlet et al. 1985). Most IVCs have intrinsically near-solar abundance (Wakker 2000). However, HVC complex C has  $A \sim 0.1$  solar (Wakker et al. 1999), and the Magellanic Stream has  $A \sim 0.25$  solar (Gibson et al. 2000). Including these HVC complexes could lower some of the apparent abundances (in 8 cases for Ca II, 4 for Fe II and 10 for Mg II), but no clear effect is visible. [An anomalously low value for Mg II, in the VHVC probed by Mrk 205, was excluded as this cloud may have low intrinsic abundance, and  $N(\text{H I})$  is uncertain.]

No distances are known for many of the HVCs/IVCs, and they fill only a small fraction of the pathlength. Thus, we looked at the relation between  $A$  and  $N(\text{H I})$ , rather than  $\langle n_{\text{H}} \rangle$ . Unexpectedly, we found tight anticorrelations of  $N(\text{H I})$  with the abundances of Mg II, Ca II, Ti II, Mn II and Fe II. A minimal correlation is expected because both quantities are integrated along lines of sight with varying physical conditions. Variations include (a) the ionization of H, (b) widely differing histories of grain destruction by interstellar shocks, and (c) considerable differences of the interstellar radiation field impinging on the gas. Ca II and Na I are not even the dominant stage of ionization in neutral regions, so the radiation field is of critical importance for their ionization fraction. In §2 we show the correlations between column density and abundances, while in §3 we discuss some implications.

## 2. Correlations between abundances and N(H I)

### 2.1. The data

Figure 1 shows scatter plots of  $\log[N(\text{H I})]$  vs  $\log[A(\text{ion})]$ , the gas-phase abundance relative to H I, for Mg II, Ca II, Ti II, Mn II, Fe II and Na I. The least-squares fit and dispersion (labeled “rms”) are given in each panel. Symbols indicate the origin of the datapoints, as detailed in the figure caption. The Local ISM points (open squares) were not used in the fits (see §2.5 below). The high-quality data obtained with the “Goddard High Resolution Spectrograph” (*GHR*S) are presented separately, in order to show the difference between halo and disk sightlines more clearly (§2.5).

The currently preferred oscillator strengths of Mn II-1197, 1201 and Mg II-1239, 1240 are 0.20 and 0.67 dex higher than those used by Jenkins et al. (1986) (see Savage & Sembach 1996a). We therefore corrected their Mn II and Mg II column densities downward by these amounts.

As the highest abundances are associated with high-velocity gas, we might be seeing a manifestation of the Routly & Spitzer (1952) effect (this is the increase in the ratio  $N(\text{Ca II})/N(\text{Na I})$  with LSR velocity). This effect is interpreted as showing that Ca is less depleted at higher peculiar velocities. However, it is based on nearby ( $<100$  pc), low-velocity ( $<20$  km s $^{-1}$ ) gas (e.g. Vallerga et al. 1993). For the HVCs/IVCs the LSR velocity is not a good measure of the peculiar velocity relative to their surroundings. Further, the IVCs for which both Na I and Ca II have been measured do not show the effect (Wakker 2000).

We now discuss some implications of the  $A$  vs  $N(\text{H I})$  relations.

### 2.2. Result 1: small dispersions

For Mg II, Mn II and Fe II the standard deviations of  $\log[A(\text{ion})]$  from the least-squares fit at a given  $N(\text{H I})$  are only 0.27 in the log. That is less than a factor 2 either way, even though the correlation extends over 4 orders of magnitude in  $N(\text{H I})$  and over 2 orders of magnitude in  $A(\text{Fe II})$ . The standard deviations are slightly larger for Ca II and Ti II (0.4 in the log, or a factor 2.6 either way). The largest scatter is seen for Na I, where it is 0.52 in the log or a factor 3.5 either way.

The larger scatter for Ca II and especially Na I may be related to the fact that, unlike the other ions, these are not the dominant ionization stage in the diffuse ISM, so that ionization effects may play a larger role. However, Ti II is the dominant ionization stage, and it shows a scatter that is comparable to that of Ca II.

Ferlet et al. (1985) proposed a slope near zero for the relation between Na I abundance and  $N(\text{H I})$  for the low-velocity gas. This has been used extensively to estimate  $N(\text{H I})$  from  $N(\text{Na I})$ . The lower column density IVC data tend to show slightly higher abundances. However, the spread in  $A(\text{Na I})$  at any given value of  $N(\text{H I})$  is rather large. For a given  $N(\text{Na I})$ , the derived  $N(\text{H I})$  will be a factor  $>3.5$  off either way in 33% of the cases. The most deviant points in the Na I diagram differ from the mean relation by a factor  $>20$ . Thus, although on average  $N(\text{Na I})/N(\text{H I})$  is independent of  $N(\text{H I})$ ,  $N(\text{Na I})$  is a rather poor predictor of  $N(\text{H I})$ .

### 2.3. Result 2: differing slopes

The slopes of the correlations differ substantially:  $-0.78 \pm 0.04$  for Ca II,  $-0.69 \pm 0.08$  for Ti II,  $-0.59 \pm 0.04$  for Fe II,  $-0.39 \pm 0.04$  for Mn II,  $-0.24 \pm 0.04$  for Mg II, and  $-0.16 \pm 0.06$  for Na I. We find slopes of  $-0.63 \pm 0.12$  and  $-0.66 \pm 0.23$  for low- and high-velocity Ca II; for Fe II we find  $-0.54 \pm 0.05$  and  $-0.70 \pm 0.07$ , respectively. For other elements there are insufficient datapoints to make separate fits. The errors are larger because of the reduced range in  $N(\text{H I})$ , but the resulting slopes are the same to within the formal error. This shows that on average the high column density, low-velocity disk gas behaves in the same manner as the low column density high-velocity halo gas.

### 2.4. Result 3: no obvious ionization effects

The ionization potentials (I.P.) of Fe II, Mn II, and Mg II are 16.2, 15.6, and 15.0 eV, respectively (compared to 13.6 eV for H I), so these ions can co-exist with  $\text{H}^+$ . The Fe III/Fe II ratio should not depend on  $N(\text{H I})$ , but only on the surrounding radiation field (which only depends on location). Thus, if the interstellar radiation field has similar values in the sightlines that were observed, and if  $\text{H}^+$  were only present in shells around H I cores, then the fraction of  $\text{H}^+$  should increase with decreasing  $N(\text{H I})$ , resulting in an overestimate of the abundance, when calculated as  $N(\text{ion})/N(\text{H I})$ . This would produce an upturn at low  $N(\text{H I})$  in the  $A$  vs  $N(\text{H I})$  relation. However, such an effect is not obvious. Ca II (I.P. 11.9 eV) should ionize more easily than H, leading to a downturn at low  $N(\text{H I})$ . This is also not seen.

### 2.5. Result 4: environmental dependence

For Mg II, Mn II and Fe II the *GHR*S disk points (open circles in Fig. 1) scatter around those of Jenkins et al. (1986). *GHR*S halo sightlines (filled circles) tend to lie above the average correlation. The small scatter in  $A(\text{Fe II})$  remarked upon by Savage & Sembach (1996a) is consistent with the fact that their halo points span only a factor 10 in  $N(\text{H I})$ . However, some more recent halo points (filled triangles) have higher Fe II/H I ratios, as do some HVCs.

The low  $N(\text{H I})$  Local ISM (LISM; open squares) shows abundances far below halo points at the same  $N(\text{H I})$ , although they are near the high end for disk gas and the observed depletion is consistent with the average Local ISM density of  $0.1 \text{ cm}^{-3}$ . We surmise that both the Sun and the LISM probes lie within a cloud, so that the LISM paths do not pass through all of it, unlike the case for clouds in the sightlines to more distant stars. Thus, the Local ISM points suggest that density is the relevant physical parameter determining depletion. Over sufficiently long pathlengths column density can substitute because it is dominated by the densest regions.

The largest depletions are seen toward  $\zeta$  Oph and  $\xi$  Per, which were used by Sembach & Savage (1996) as the archetypical cold disk sightlines. These have high  $N(\text{H I})$  and  $A(\text{Mg II})$  and  $A(\text{Fe II})$  lie below the average relation. Including  $N(\text{H}_2)$  would move these points 0.2 and 0.4 dex to the right and down, respectively, shifting them  $\sim 0.1$  and 0.2 dex further below the average.

We thus see the environmental dependence found by Sembach & Savage (1996): disk sightlines tend to have low gas-phase abundances, while halo sightlines show high gas-phase abundances. We can understand this in large part as a column density dependence, as disk sightlines tend to have higher column density than halo sightlines.

### 3. Discussion

The general trend that the gas phase abundances of refractory ions decreases with  $N(\text{H I})$  is, of course, well known; the ions are removed from the gas phase by sticking to grains. *However, the low dispersions of the depletions at a particular value of  $N(\text{H I})$ , continuing to low values to  $N(\text{H I})$ , are remarkable.* The depletion patterns provide a diagnostic of the density fluctuation within the ISM, since the depletions require encounters between the grains and ions. *The low dispersions of  $A$  at a given  $N(\text{H I})$  suggest additional properties of the ISM:*

1. Large values of  $N(\text{H I})$  arise from one or a few regions of relatively large local density rather than from a superposition of many regions of lower density. In this way, there is unexpected physical meaning to the integrated column density: a good correlation with the mean *local* density of the typical H atom along the sightline. If large values of  $N(\text{H I})$  were built up from many regions of low density along the line of sight, the averaged  $A$  would correspond to the lower densities. The association of large  $N(\text{H I})$  with a large local density is strengthened by the fact that the anticorrelation of gas phase abundances with  $\langle n_{\text{H}} \rangle$  is better than with  $N(\text{H I})$  (Savage & Bohlin 1979).

2. The low dispersions in  $\log[A]$  suggest that grains are not destroyed in strong shocks, as some models have suggested. If such destruction occurred, a few points with large gas phase abundances would be expected at large  $N(\text{H I})$ . Rather, the detachment of a refractory element from grains seems to be a continuous function of the mean density, and is common enough to produce a low dispersion about the mean. Grain destruction may occur by means of many small shocks with a broad distribution of velocities.

3. Both the rates of ions sticking to grains and becoming detached from them (probably in atomic form) must be rapid enough to achieve rather good statistical equilibrium. These balancing rates lead to a particular value of  $A$  for a given density; otherwise, the past history of the H I along the line of sight would strongly influence  $A$ .

4. In view of (3) above, we think that the best possibility is that attachment takes place within regions of far greater than average density distributed along each line of sight. Encounters between grains and ions are very slow if the mean density of the diffuse ISM is assumed (see below). Possibly magnetohydrodynamic waves create non-thermal motions of the ions relative to the grains, since the charge per mass of the grains is vastly less than for the ions. As a result, ions encounter more dust grains and the net attachment rate increases.

Under the assumption that relative motions were thermal, Weingartner & Draine (1999) calculated average gas phase abundances of a highly depleted species (Ti II) for large  $N(\text{H I})$ . In their model, dense ( $\langle n_{\text{H}} \rangle \sim 10^3 \text{ cm}^{-3}$ ) molecular clouds contain half the mass of the ISM, 30% is in

cool, neutral clouds ( $\langle n_{\text{H}} \rangle = 30 \text{ cm}^{-3}$ ) and 20% is in warm neutral clouds ( $\langle n_{\text{H}} \rangle = 0.4 \text{ cm}^{-3}$ ). The attachment of the Ti onto grains occurs in the molecular and cool clouds. This model shows that the observed  $A(\text{Ti II})$  for large  $N(\text{H I})$  can only be achieved by circulation into very dense regions. To achieve rapid attachment within the diffuse ISM, such circulation seems necessary, operating at both low and high column densities. An additional condition for rapid attachment of ions is that the gas be cold as well as dense, in order to provide efficient focusing by the Coulomb force onto negatively charged grains.

We appreciate comments and clarifications by an anonymous referee, Alex Lazarian, Chris Howk, and Bruce Draine. B.P.W. is partially supported by NASA grant NAG5-9179.

### REFERENCES

- Anders, E., Grevesse, N. 1989, *Geochim. Cosmochim. Acta*, 53, 197
- Cardelli, J.A., Sembach, K.R., & Savage, B.D. 1995, *ApJ*, 440, 241
- Crinklaw, G., Federman, S.R., & Joseph, C.L. 1994, *ApJ*, 424, 748
- Ferlet, R., Vidal-Madjar, A., & Gry, C. 1985, *ApJ*, 298, 838
- Fitzpatrick, E.L., & Spitzer, L. 1997, *ApJ*, 475, 623
- Gibson, B.K., Giroux, M.L., Penton, S.V., Putman, M.E., Stocke, J.T., Shull, M.J. 2000a, *AJ*, accepted, astro-ph/0007078
- Hébrard, G., Mallouris, C., Ferlet, R., Koester, D., Lemoine, M., Vidal-Madjar, A., York, D. 1999, *A&A*, 350, 643
- Howk, J.C., Savage, B.D., & Fabian, D. 1999, *ApJ*, 525, 253
- Kuntz, K.D., & Danly, L. 1996, *ApJ*, 457, 703
- Jenkins, E.B., Savage, B.D., & Spitzer, L. 1986, *ApJ*, 301, 355
- Linsky, J.L., Diplas, A., Wood, B.E., Brown, A., Ayres, T., Savage, B.D. 1995, *ApJ*, 451, 335
- Routly, P.M., Spitzer, L. 1952, *ApJ*, 115, 227
- Savage, B.D., Lu, L., Weymann, R., Morris, S., & Gilliland, R. 1993, *ApJ*, 404, 124
- Savage, B.D., & Bohlin, R.C. 1979, *ApJ*, 229, 136
- Savage, B.D., & Sembach, K.R. 1996a, *ARAA*, 34, 279
- Savage, B.D., & Sembach, K.R. 1996b *ApJ*, 470, 893

- Sembach, K.,R., & Savage, B.D. 1996, ApJ, 457, 211
- Sofia, U.J., Cardelli, J.A., & Savage, B.D. 1994, ApJ, 430, 650
- Spitzer, L. 1985, ApJ, 290, L21
- Spitzer, L., & Fitzpatrick E.L. 1995, ApJ, 445, 196
- Vallerga, J.V., Vedder, P.W., Craig, N., Welsh, B.Y. 1993, ApJ, 411, 729
- Wakker, B.P., Howk, C., Savage, B.D., Tufte, S.L., Reynolds, R.J., van Woerden, H., Schwarz, U.J., Peletier, R.F., Kalberla, P.M.W. 1999, Nature, 400, 388
- Wakker, B.P., & van Woerden, H. 1997, ARAA, 5, 217
- Wakker, B.P. 2000, ApJS, submitted
- Weingartner, J.C., & Draine, B.T. 1999, ApJ, 517, 292

Figure 1. Correlation plots of the abundances of Na I, Mg II, Ca II, Ti II, Mn II and Fe II vs N(H I). The solid lines show the least-squares fits, whose coefficients are given by the label in the lower left corner. “rms” is the rms of the residual, also indicated by the two parallel dotted lines. “ $\rho$ ” is the correlation coefficient. Filled circles are for the HVC and IVC data from Wakker (2000). If measurement errors were given for N(ion), error bars are shown; usually no errors are available. Crosses show data for low-velocity gas from Ferlet et al. (1985; Na I), Jenkins et al. (1986; Mg II, Mn II and Fe II) and Crinklaw et al. (1994; Ca II, Ti II). Errors are usually smaller than the size of the dot. The right panels for Mg II, Mn II and Fe II separately show measurements with relatively low systematic errors obtained with the *GHRIS* by Savage et al. (1993), Sofia et al. (1994), Cardelli et al. (1995), Spitzer & Fitzpatrick (1995), Savage & Sembach (1996b) and Sembach & Savage (1996). For these data, halo sightlines are shown by filled circles, disk sightlines by open circles. Filled/open triangles show halo/disk sightlines from Fitzpatrick & Spitzer (1997; after combining their fit components into the 5 H I components visible in the spectrum) and Howk et al. (1999). Open squares show Local ISM sightlines from Linsky et al. (1995), Hébrard et al. (1999) and Howk (priv. comm.); these were not used in the fits, see §2.4. For all low-velocity data the error bars are smaller than the symbol sizes. The horizontal lines show the solar reference abundance, from Anders & Grevesse (1989).



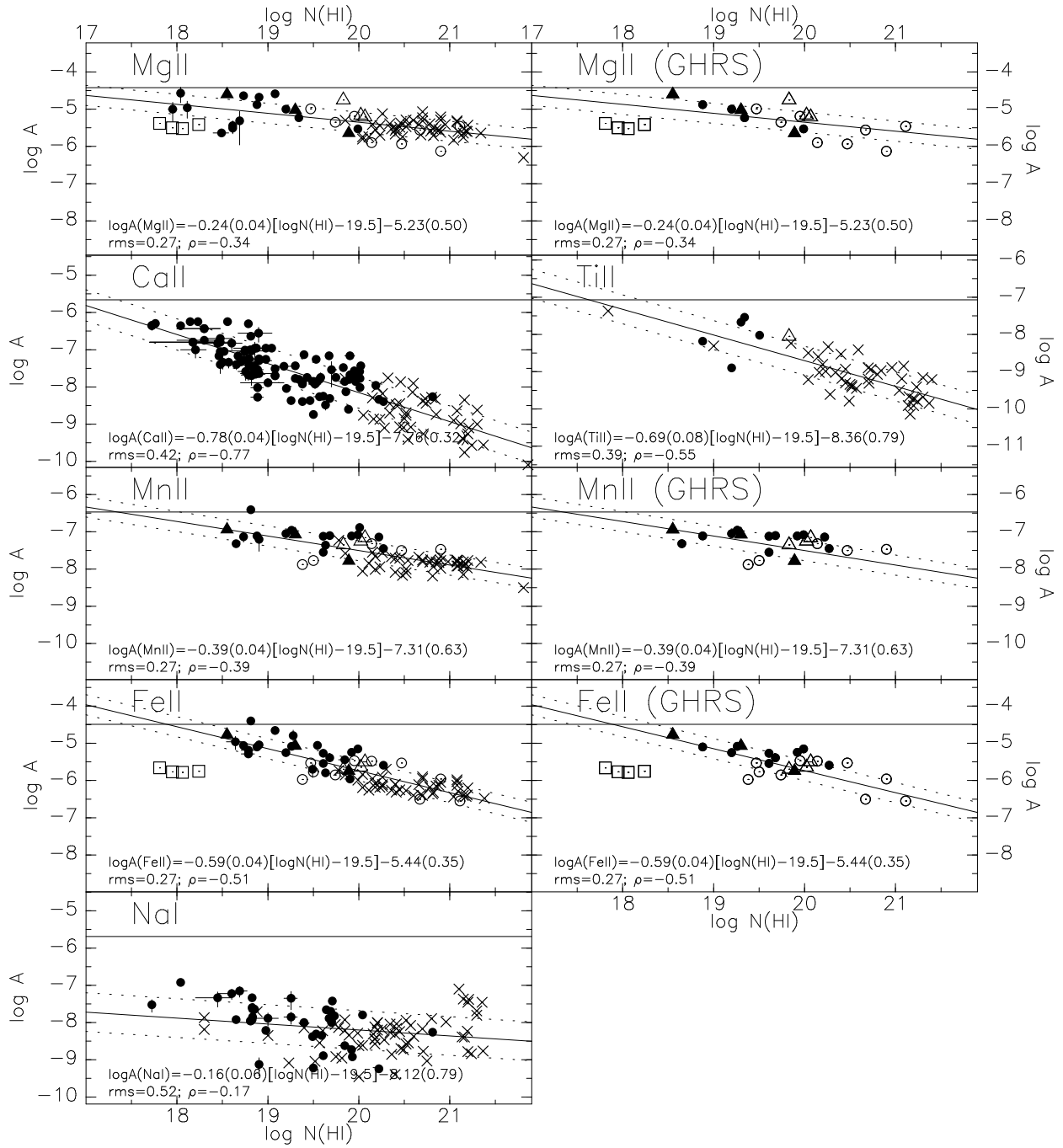


Figure 1

## DEPENDENCE OF GAS PHASE ABUNDANCES IN THE ISM ON COLUMN DENSITY

B.P. WAKKER, J.S. MATHIS

Department of Astronomy, University of Wisconsin  
475 N Charter St, Madison, WI53706, USA  
wakker@astro.wisc.edu, mathis@astro.wisc.edu*Draft version September 25, 2000*

## ABSTRACT

Sightlines through high- and intermediate-velocity clouds allow measurements of ionic gas phase abundances,  $A$ , at very low values of H I column density,  $N(\text{H I})$ . Present observations cover over 4 orders of magnitude in  $N(\text{H I})$ . Remarkably, for several ions we find that the  $A$  vs  $N(\text{H I})$  relation is the same at high and low column density and that the abundances have a relatively low dispersion (factors of 2–3) at any particular  $N(\text{H I})$ . Halo gas tends to have slightly higher values of  $A$  than disk gas at the same  $N(\text{H I})$ , suggesting that part of the dispersion may be attributed to the environment. We note that the dispersion is largest for Na I; using Na I as a predictor of  $N(\text{H I})$  can lead to large errors.

Important implications of the low dispersions regarding the physical nature of the ISM are: (a) because of clumping, over sufficiently long pathlengths  $N(\text{H I})$  is a reasonable measure of the *local* density of *most* of the H atoms along the sight line; (b) the destruction of grains does not mainly take place in catastrophic events such as strong shocks, but is a continuous function of the mean density; (c) the cycling of the ions becoming attached to grains and being detached must be rapid, and the two rates must be roughly equal under a wide variety of conditions; (d) in gas that has a low average density the attachment should occur within denser concentrations.

*Subject headings:* ISM: clouds, ISM, Abundances Galaxy: halo, Galaxy: disk

## 1. INTRODUCTION

The study of elemental abundances in the interstellar medium has a long history, both in the optical and with space-based UV spectrographs, such as *Copernicus* and the Hubble Space Telescope (*HST*). These studies show that most elements have apparent abundances relative to hydrogen substantially below those in the Sun. This is interpreted as due to depletion of ions onto dust grains.

Savage & Sembach (1996a) summarized high-quality abundance studies based on *HST* data. They concluded that the depletion of an element depends on the nature of the interstellar medium along the sightline. In cold, dense disk gas, S has near-solar abundance, while Si, Mg, Mn, Cr, Fe and Ni are progressively more depleted. In warm-disk gas, the gas-phase abundances appear higher than in the cool gas, while in halo gas they are even larger.

Jenkins, Savage & Spitzer (1986) used *Copernicus* to measure accurate column densities for Mg II, P II, Cl I, Cl II, Mn II and Fe II, for stars with distances,  $d$ , between 0.1 and 2 kpc. They measured  $N(\text{H I})$  from the damping wings of Ly $\alpha$  and found a relation between the ionic abundance relative to H I,  $A$ , and the average density,  $\langle n_{\text{H}} \rangle$  ( $\equiv N(\text{H I})/d$ ). An explanation was provided by Spitzer (1985), who suggested that the observed depletion in a line of sight depends on the fraction of warm and cold (dense) gas encountered, where each component has a specific gas phase abundance of each ion.

Crinklaw, Federman, & Joseph (1994) observed Ca II and Ti II toward 12 stars with distances between 150 and 650 pc. The slope of the relation between  $\log[\langle n_{\text{H}} \rangle]$  and  $\log[A(\text{ion})]$  is similar for Ca II and Ti II, but it differs from those for Fe II, Mn II, Mg II and P II. They proposed that Ca II and Ti II mostly occur in the warm intercloud

medium, and that the apparent depletion is very sensitive to the inclusion of high-density regions (with high depletion) in the sightline.

These studies were limited to sightlines with  $N(\text{H I})$  in the range  $10^{20}$  to  $7 \times 10^{21} \text{ cm}^{-2}$ . To extend this range, we used the high- and intermediate-velocity gas (HVCs and IVCs, see Kuntz & Danly 1996, Wakker & van Woerden 1997, Wakker 2000). In 21-cm emission these stand out in velocity from gas in the Milky Way disk, so that weak components (down to  $10^{18} \text{ cm}^{-2}$ ) can be measured. At low velocities, parcels of gas with such low column densities can not be separated from other high column density concentrations in the line of sight.

Wakker (2000) analyzed all the published absorption-line data pertaining to the high- and intermediate-velocity gas. Improved H I column densities (and thus improved ion abundances) were determined for about 250 sightlines. Ca II was measured for 97 components, Ti II for 6, Fe II for 13, Mn II for 5, Mg II for 10, and Na I for 34 (low-velocity Na I was taken from Ferlet et al. 1985). Most IVCs have intrinsically near-solar abundance (Wakker 2000). However, HVC complex C has  $A \sim 0.1$  solar (Wakker et al. 1999), and the Magellanic Stream has  $A \sim 0.25$  solar (Gibson et al. 2000). Including these HVC complexes could lower some of the apparent abundances (in 8 cases for Ca II, 4 for Fe II and 10 for Mg II), but no clear effect is visible. [An anomalously low value for Mg II, in the VHVC probed by Mrk 205, was excluded as this cloud may have low intrinsic abundance, and  $N(\text{H I})$  is uncertain.]

No distances are known for many of the HVCs/IVCs, and they fill only a small fraction of the pathlength. Thus, we looked at the relation between  $A$  and  $N(\text{H I})$ , rather than  $\langle n_{\text{H}} \rangle$ . Unexpectedly, we found tight anticorrelations of  $N(\text{H I})$  with the abundances of Mg II, Ca II, Ti II, Mn II

and Fe II. A minimal correlation is expected because both quantities are integrated along lines of sight with varying physical conditions. Variations include (a) the ionization of H, (b) widely differing histories of grain destruction by interstellar shocks, and (c) considerable differences of the interstellar radiation field impinging on the gas. Ca II and Na I are not even the dominant stage of ionization in neutral regions, so the radiation field is of critical importance for their ionization fraction. In Sect. 2 we show the correlations between column density and abundances, while in Sect. 3 we discuss some implications.

## 2. CORRELATIONS BETWEEN ABUNDANCES AND N(H I)

### 2.1. The data

Figure 1 shows scatter plots of  $\log[N(\text{H I})]$  vs  $\log[A(\text{ion})]$ , the gas-phase abundance relative to H I, for Mg II, Ca II, Ti II, Mn II, Fe II and Na I. The least-squares fit and dispersion (labeled “rms”) are given in each panel. Symbols indicate the origin of the datapoints, as detailed in the figure caption. The Local ISM points (open squares) were not used in the fits (see Sect. 2.5 below). The high-quality data obtained with the “Goddard High Resolution Spectrograph” (*GHR*S) are presented separately, in order to show the difference between halo and disk sightlines more clearly (Sect. 2.5).

The currently preferred oscillator strengths of Mn II-1197, 1201 and Mg II-1239, 1240 are 0.20 and 0.67 dex higher than those used by Jenkins et al. (1986) (see Savage & Sembach 1996a). We therefore corrected their Mn II and Mg II column densities downward by these amounts.

As the highest abundances are associated with high-velocity gas, we might be seeing a manifestation of the Routly & Spitzer (1952) effect (this is the increase in the ratio  $N(\text{Ca II})/N(\text{Na I})$  with LSR velocity). This effect is interpreted as showing that Ca is less depleted at higher peculiar velocities. However, it is based on nearby (<100 pc), low-velocity (<20 km s<sup>-1</sup>) gas (e.g. Vallerga et al. 1993). For the HVCs/IVCs the LSR velocity is not a good measure of the peculiar velocity relative to their surroundings. Further, the IVCs for which both Na I and Ca II have been measured do not show the effect (Wakker 2000).

We now discuss some implications of the  $A$  vs  $N(\text{H I})$  relations.

### 2.2. Result 1: small dispersions

For Mg II, Mn II and Fe II the standard deviations of  $\log[A(\text{ion})]$  from the least-squares fit at a given  $N(\text{H I})$  are only 0.27 in the log. That is less than a factor 2 either way, even though the correlation extends over 4 orders of magnitude in  $N(\text{H I})$  and over 2 orders of magnitude in  $A(\text{Fe II})$ . The standard deviations are slightly larger for Ca II and Ti II (0.4 in the log, or a factor 2.6 either way). The largest scatter is seen for Na I, where it is 0.52 in the log or a factor 3.5 either way.

The larger scatter for Ca II and especially Na I may be related to the fact that, unlike the other ions, these are not the dominant ionization stage in the diffuse ISM, so that ionization effects may play a larger role. However, Ti II is the dominant ionization stage, and it shows a scatter that is comparable to that of Ca II.

Ferlet et al. (1985) proposed a slope near zero for the relation between Na I abundance and  $N(\text{H I})$  for the low-velocity gas. This has been used extensively to estimate  $N(\text{H I})$  from  $N(\text{Na I})$ . The lower column density IVC data tend to show slightly higher abundances. However, the spread in  $A(\text{Na I})$  at any given value of  $N(\text{H I})$  is rather large. For a given  $N(\text{Na I})$ , the derived  $N(\text{H I})$  will be a factor >3.5 off either way in 33% of the cases. The most deviant points in the Na I diagram differ from the mean relation by a factor >20. Thus, although on average  $N(\text{Na I})/N(\text{H I})$  is independent of  $N(\text{H I})$ ,  $N(\text{Na I})$  is a rather poor predictor of  $N(\text{H I})$ .

### 2.3. Result 2: differing slopes

The slopes of the correlations differ substantially:  $-0.78 \pm 0.04$  for Ca II,  $-0.69 \pm 0.08$  for Ti II,  $-0.59 \pm 0.04$  for Fe II,  $-0.39 \pm 0.04$  for Mn II,  $-0.24 \pm 0.04$  for Mg II, and  $-0.16 \pm 0.06$  for Na I. We find slopes of  $-0.63 \pm 0.12$  and  $-0.66 \pm 0.23$  for low- and high-velocity Ca II; for Fe II we find  $-0.54 \pm 0.05$  and  $-0.70 \pm 0.07$ , respectively. For other elements there are insufficient datapoints to make separate fits. The errors are larger because of the reduced range in  $N(\text{H I})$ , but the resulting slopes are the same to within the formal error. This shows that on average the high column density, low-velocity disk gas behaves in the same manner as the low column density high-velocity halo gas.

### 2.4. Result 3: no obvious ionization effects

The ionization potentials (I.P.) of Fe II, Mn II, and Mg II are 16.2, 15.6, and 15.0 eV, respectively (compared to 13.6 eV for H I), so these ions can co-exist with H<sup>+</sup>. The Fe III/Fe II ratio should not depend on  $N(\text{H I})$ , but only on the surrounding radiation field (which only depends on location). Thus, if the interstellar radiation field has similar values in the sightlines that were observed, and if H<sup>+</sup> were only present in shells around H I cores, then the fraction of H<sup>+</sup> should increase with decreasing  $N(\text{H I})$ , resulting in an overestimate of the abundance, when calculated as  $N(\text{ion})/N(\text{H I})$ . This would produce an upturn at low  $N(\text{H I})$  in the  $A$  vs  $N(\text{H I})$  relation. However, such an effect is not obvious. Ca II (I.P. 11.9 eV) should ionize more easily than H, leading to a downturn at low  $N(\text{H I})$ . This is also not seen.

### 2.5. Result 4: environmental dependence

For Mg II, Mn II and Fe II the *GHR*S disk points (open circles in Fig. 1) scatter around those of Jenkins et al. (1986). *GHR*S halo sightlines (filled circles) tend to lie above the average correlation. The small scatter in  $A(\text{Fe II})$  remarked upon by Savage & Sembach (1996a) is consistent with the fact that their halo points span only a factor 10 in  $N(\text{H I})$ . However, some more recent halo points (filled triangles) have higher Fe II/H I ratios, as do some HVCs.

The low  $N(\text{H I})$  Local ISM (LISM; open squares) shows abundances far below halo points at the same  $N(\text{H I})$ , although they are near the high end for disk gas and the observed depletion is consistent with the average Local ISM density of 0.1 cm<sup>-3</sup>. We surmise that both the Sun and the LISM probes lie within a cloud, so that the LISM paths do not pass through all of it, unlike the case for clouds in the sightlines to more distant stars. Thus, the Local

ISM points suggest that density is the relevant physical parameter determining depletion. Over sufficiently long pathlengths column density can substitute because it is dominated by the densest regions.

The largest depletions are seen toward  $\zeta$  Oph and  $\xi$  Per, which were used by Sembach & Savage (1996) as the archetypical cold disk sightlines. These have high N(H I) and A(Mg II) and A(Fe II) lie below the average relation. Including N(H<sub>2</sub>) would move these points 0.2 and 0.4 dex to the right and down, respectively, shifting them  $\sim 0.1$  and 0.2 dex further below the average.

We thus see the environmental dependence found by Sembach & Savage (1996): disk sightlines tend to have low gas-phase abundances, while halo sightlines show high gas-phase abundances. We can understand this in large part as a column density dependence, as disk sightlines tend to have higher column density than halo sightlines.

### 3. DISCUSSION

The general trend that the gas phase abundances of refractory ions decreases with N(H I) is, of course, well known; the ions are removed from the gas phase by sticking to grains. *However, the low dispersions of the depletions at a particular value of N(H I), continuing to low values to N(H I), are remarkable.* The depletion patterns provide a diagnostic of the density fluctuation within the ISM, since the depletions require encounters between the grains and ions. *The low dispersions of A at a given N(H I) suggest additional properties of the ISM:*

1. Large values of N(H I) arise from one or a few regions of relatively large local density rather than from a superposition of many regions of lower density. In this way, there is unexpected physical meaning to the integrated column density: a good correlation with the mean *local* density of the typical H atom along the sightline. If large values of N(H I) were built up from many regions of low density along the line of sight, the averaged *A* would correspond to the lower densities. The association of large N(H I) with a large local density is strengthened by the fact that the anticorrelation of gas phase abundances with  $\langle n_{\text{H}} \rangle$  is better than with N(H I) (Savage & Bohlin 1979).

2. The low dispersions in  $\log[A]$  suggest that grains are not destroyed in strong shocks, as some models have suggested. If such destruction occurred, a few points with

large gas phase abundances would be expected at large N(H I). Rather, the detachment of a refractory element from grains seems to be a continuous function of the mean density, and is common enough to produce a low dispersion about the mean. Grain destruction may occur by means of many small shocks with a broad distribution of velocities.

3. Both the rates of ions sticking to grains and becoming detached from them (probably in atomic form) must be rapid enough to achieve rather good statistical equilibrium. These balancing rates lead to a particular value of *A* for a given density; otherwise, the past history of the H I along the line of sight would strongly influence *A*.

4. In view of (3) above, we think that the best possibility is that attachment takes place within regions of far greater than average density distributed along each line of sight. Encounters between grains and ions are very slow if the mean density of the diffuse ISM is assumed (see below). Possibly magnetohydrodynamic waves create non-thermal motions of the ions relative to the grains, since the charge per mass of the grains is vastly less than for the ions. As a result, ions encounter more dust grains and the net attachment rate increases.

Under the assumption that relative motions were thermal, Weingartner & Draine (1999) calculated average gas phase abundances of a highly depleted species (Ti II) for large N(H I). In their model, dense ( $\langle n_{\text{H}} \rangle \sim 10^3 \text{ cm}^{-3}$ ) molecular clouds contain half the mass of the ISM, 30% is in cool, neutral clouds ( $\langle n_{\text{H}} \rangle = 30 \text{ cm}^{-3}$ ) and 20% is in warm neutral clouds ( $\langle n_{\text{H}} \rangle = 0.4 \text{ cm}^{-3}$ ). The attachment of the Ti onto grains occurs in the molecular and cool clouds. This model shows that the observed *A*(Ti II) for large N(H I) can only be achieved by circulation into very dense regions. To achieve rapid attachment within the diffuse ISM, such circulation seems necessary, operating at both low and high column densities. An additional condition for rapid attachment of ions is that the gas be cold as well as dense, in order to provide efficient focusing by the Coulomb force onto negatively charged grains.

We appreciate comments and clarifications by an anonymous referee, Alex Lazarian, Chris Howk, and Bruce Draine. B.P.W. is partially supported by NASA grant NAG5-9179.

### REFERENCES

- Anders, E., Grevesse, N. 1989, *Geochim. Cosmochim. Acta*, 53, 197  
 Cardelli, J.A., Sembach, K.R., & Savage, B.D. 1995, *ApJ*, 440, 241  
 Crinklaw, G., Federman, S.R., & Joseph, C.L. 1994, *ApJ*, 424, 748  
 Ferlet, R., Vidal-Madjar, A., & Gry, C. 1985, *ApJ*, 298, 838  
 Fitzpatrick, E.L., & Spitzer, L. 1997, *ApJ*, 475, 623  
 Gibson, B.K., Giroux, M.L., Penton, S.V., Putman, M.E., Stocke, J.T., Shull, M.J. 2000a, *AJ*, accepted, astro-ph/0007078  
 Hébrard, G., Mallouris, C., Ferlet, R., Koester, D., Lemoine, M., Vidal-Madjar, A., York, D. 1999, *A&A*, 350, 643  
 Howk, J.C., Savage, B.D., & Fabian, D. 1999, *ApJ*, 525, 253  
 Kuntz, K.D., & Danly, L. 1996, *ApJ*, 457, 703  
 Jenkins, E.B., Savage, B.D., & Spitzer, L. 1986, *ApJ*, 301, 355  
 Linsky, J.L., Diplas, A., Wood, B.E., Brown, A., Ayres, T., Savage, B.D. 1995, *ApJ*, 451, 335  
 Routly, P.M., Spitzer, L. 1952, *ApJ*, 115, 227  
 Savage, B.D., Lu, L., Weymann, R., Morris, S., & Gilliland, R. 1993, *ApJ*, 404, 124  
 Savage, B.D., & Bohlin, R.C. 1979, *ApJ*, 229, 136  
 Savage, B.D., & Sembach, K.R. 1996a, *ARAA*, 34, 279  
 Savage, B.D., & Sembach, K.R. 1996b, *ApJ*, 470, 893  
 Sembach, K.R., & Savage, B.D. 1996, *ApJ*, 457, 211  
 Sofia, U.J., Cardelli, J.A., & Savage, B.D. 1994, *ApJ*, 430, 650  
 Spitzer, L. 1985, *ApJ*, 290, L21  
 Spitzer, L., & Fitzpatrick E.L. 1995, *ApJ*, 445, 196  
 Vallerga, J.V., Vedder, P.W., Craig, N., Welsh, B.Y. 1993, *ApJ*, 411, 729  
 Wakker, B.P., Howk, C., Savage, B.D., Tufte, S.L., Reynolds, R.J., van Woerden, H., Schwarz, U.J., Peletier, R.F., Kalberla, P.M.W. 1999, *Nature*, 400, 388  
 Wakker, B.P., & van Woerden, H. 1997, *ARAA*, 5, 217  
 Wakker, B.P. 2000, *ApJS*, submitted  
 Weingartner, J.C., & Draine, B.T. 1999, *ApJ*, 517, 292

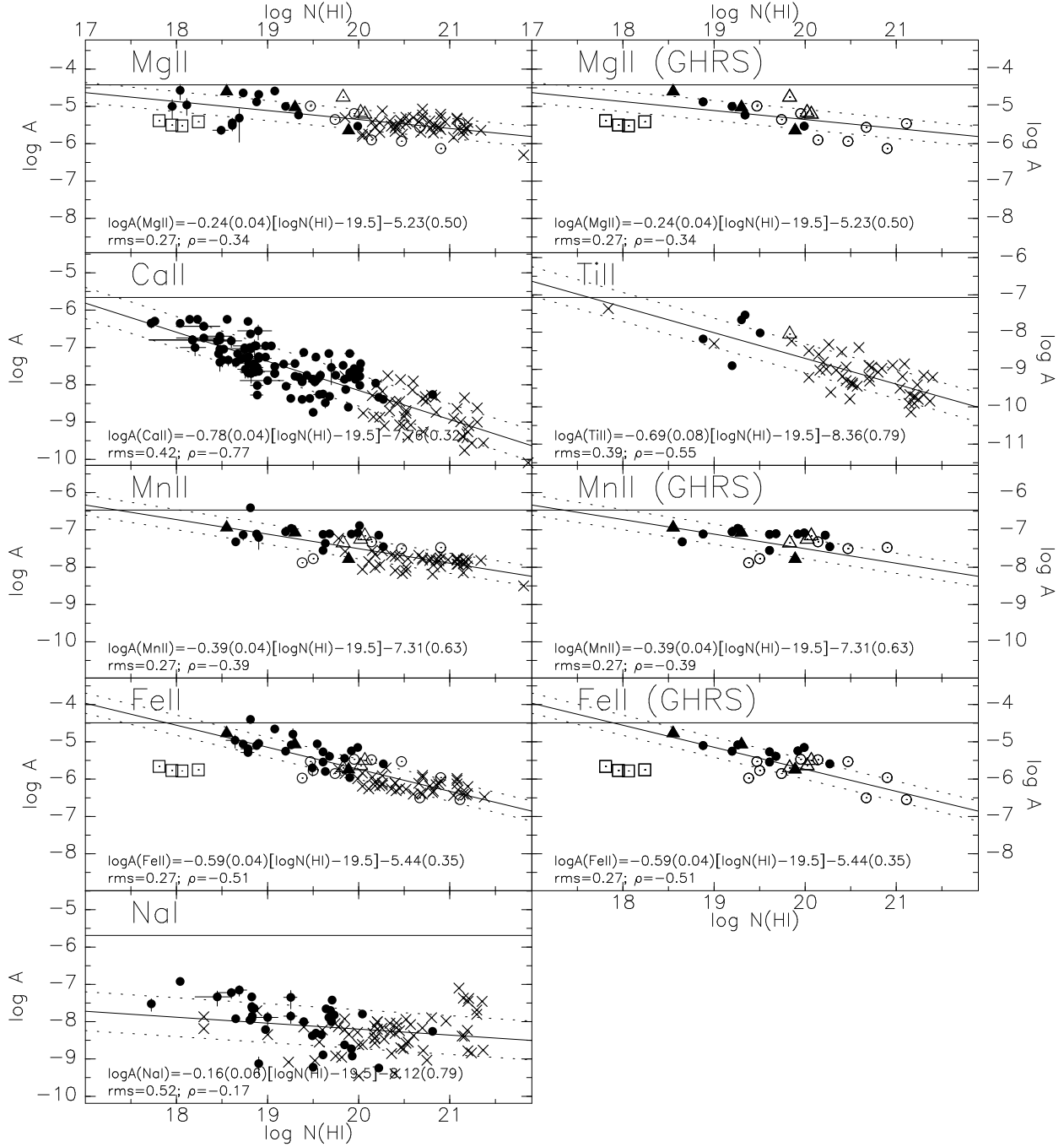


Figure 1. Correlation plots of the abundances of Na I, Mg II, Ca II, Ti II, Mn II and Fe II vs  $N(\text{H I})$ . The solid lines show the least-squares fits, whose coefficients are given by the label in the lower left corner. “rms” is the rms of the residual, also indicated by the two parallel dotted lines. “ $\rho$ ” is the correlation coefficient. Filled circles are for the HVC and IVC data from Wakker (2000). If measurement errors were given for  $N(\text{ion})$ , error bars are shown; usually no errors are available. Crosses show data for low-velocity gas from Ferlet et al. (1985; Na I), Jenkins et al. (1986; Mg II, Mn II and Fe II) and Crinklaw et al. (1994; Ca II, Ti II). Errors are usually smaller than the size of the dot. The right panels for Mg II, Mn II and Fe II separately show measurements with relatively low systematic errors obtained with the *GHRIS* by Savage et al. (1993), Sofia et al. (1994), Cardelli et al. (1995), Spitzer & Fitzpatrick (1995), Savage & Sembach (1996b) and Sembach & Savage (1996). For these data, halo sightlines are shown by filled circles, disk sightlines by open circles. Filled/open triangles show halo/disk sightlines from Fitzpatrick & Spitzer (1997; after combining their fit components into the 5 H I components visible in the spectrum) and Howk et al. (1999). Open squares show Local ISM sightlines from Linsky et al. (1995), Hébrard et al. (1999) and Howk (priv. comm.); these were not used in the fits, see Sect. 2.4. For all low-velocity data the error bars are smaller than the symbol sizes. The horizontal lines show the solar reference abundance, from Anders & Grevesse (1989).